Chemistry and Materials

The Center for Science Innovation

Research Article

Chem. Mater. 2 (3) 2023, 77-81

Enhancing Antioxidant Activity of Curcumin Using ZnO Nanoparticles Synthesized by Electrodeposition Method

Nisrina Fitri Nur Syamsi*, Alsifa Andita Putri, Devia Alventiana Sipayung, Rachmaniah Nurul Imani, Suci Putriyaningsih, Anis Sakinah

Department of Chemistry, Faculty of Mathematics and Natural Science, Universitas Negeri Jakarta, Jl. Rawamangun Muka, Jakarta 13220, Indonesia

*Corresponding author: nisrinafitrinur@gmail.com

Received
18 September 2023

Received in revised form
20 October 2023

Accepted
24 October 2023

Published online
31 October 2023

DOI
https://doi.org/10.56425/cma.v2i3.68

Abstract

The objective of this study was to fabricate zinc oxide (ZnO) nanoparticles through the utilization of the electrodeposition technique, to employ them as a supportive medium for enhancing the antioxidant properties of curcumin. The study involved the synthesis of ZnO nanoparticles, which were subsequently subjected to characterization using X-ray diffraction (XRD), scanning electron microscopy (SEM), and electrochemical impedance spectroscopy (EIS). Additionally, the antioxidant activity of the synthesized nanoparticles was assessed through the use of the 2,2-diphenyl-1-picrylhydrazyl (DPPH) method. In XRD analysis, a notable peak denoted by an asterisk (*) is observed at specific angles of 2θ: 25.84°, 31.63°, 34.21°, and 36.12°, with corresponding index values (h, k, l) of (220), (100), (002), and (101), respectively. This peak is indicative of the degree of crystallinity exhibited by ZnO nanoparticles. The SEM data indicates that the particles generated possess a rod-like morphology, exhibiting a range of sizes. The Nyquist plots exhibit a semicircular arc pattern at low frequencies, as indicated by the findings from the EIS test. The data obtained from antioxidant assays indicated that ZnO-curcumin achieved an inhibition level of 47.09%, while curcumin alone showed a significantly lower inhibition percentage of 4.93%.

Keywords: curcumin, antioxidant, ZnO nanoparticles.

1. Introduction

Free radicals as unstable atoms, molecules, or molecular fragments can damage body cells and cause oxidative stress resulting in health problems, including premature aging and other degenerative diseases [1]. Antioxidants can inhibit oxidative damage through reactions with free radicals indirectly by inhibiting the activity or expression of free radical-producing enzymes and increasing the activity of intracellular enzymes. Antioxidants are classified into two groups, synthetic and natural antioxidants. Synthetic antioxidants, such as butylated hydroxyanisole (BHA), butylated hydroxytoluene (BHT), propyl gallate (PG), while natural antioxidants derived from plants are classified into three main classes, such as phenolic compounds, vitamins, and carotenoids. Limitations resulting from natural antioxidants include susceptibility to degradation, low permeability, poor water solubility, and instability during the storage process [2]. Similarly, synthetic antioxidants, are known to be responsible for having adverse effects on the liver and potentially causing carcinogenesis [3].

Research that has been conducted shows that curcumin in Curcuma longa has potential as an antioxidant. Curcumin can interact with various molecular mechanisms to reduce the level of oxidative stress, including the ability to chelate heavy metals or regulate enzyme activity [4]. However, several studies showed that curcumin results in low bioactivity, poor absorption, rapid metabolism, and chemical instability [5,6]. Therefore, it is necessary to improve the biocompatibility and bioactivity of antioxidants with nanotechnology which has previously been widely developed and proven to have advantages in various fields [7].

Nanoparticles are effective candidates to support curcumin bioactivity because they have distinctive mechanical, thermal, and optical properties and produce a

larger surface area. Nanoparticles functionalized with natural antioxidants act as targeted delivery systems to enhance antioxidant activity [7]. This statement is supported by research conducted by Ge *et al.* proving that nanoparticles functionalized with antioxidants produce effective antioxidant activity[8].

The characteristics of zinc oxide (ZnO) nanoparticles are interesting to study because they have properties such as biocompatibility and lack of toxicity, making ZnO nanoparticles a desirable alternative for the development of biological applications and can be used safely in biomedical applications [9]. ZnO nanoparticles have been found to exhibit toxicological activities such as cytotoxicity, genotoxicity, and free radical activity in vitro. Arasu *et al.* have succeeded in synthesizing ZnO/C which has antioxidant activity [10]. ZnO nanoparticles as a support agent for curcumin are expected to provide a more optimal quality of antioxidant activity. The size of the nanoparticles has a significant impact on the surface area of the material because they have more contact points and interactions with the environment free radicals [11].

ZnO nanoparticles can be synthesized using the electrodeposition method. Liu *et al.* have succeeded in synthesizing ZnO nanoparticles by electrodeposition method [12]. The ZnO film morphology can be designed with various experimental parameters, such as potential voltage, electrolyte concentration, deposition time, and temperature. This work aimed to synthesize ZnO nanoparticles using the electrodeposition method as a supporting material for curcumin's antioxidant activity.

2. Materials and Method

The materials used were $HAuCl_4$, $Zn(NO_3)_2$ (Merck), indium tin oxide (ITO) substrate, KCl (Merck), Curcumin (Merck), 2,2-diphenyl-picrylhydrazyl (Sigma Aldrich), and analytical ethanol (Merck).

ZnO nanoparticles were synthesized using the electrodeposition technique. The precursor used was $Zn(NO_3)_2$ 0.5 M. Subsequently, an electrodeposition setup was prepared with a three-electrode system, where the ITO served as the working electrode for depositing ZnO nanoparticles, Ag/AgCl as the reference electrode, and platinum (Pt) as the counter electrode. The synthesis was carried out at a temperature of 40°C for 60 minutes, with the potential set at -1.0 V.

The particle size and crystal structure analysis of ZnO nanoparticles were conducted using an X-ray diffractometer (XRD, PANalytical AERIS). The samples characterized using XRD were ZnO films deposited on ITO substrates. Measurement result curves in the form of diffraction peaks from diffraction fields at position 2θ, representing diffraction fields in specific directions, were processed using X'Pert High Score Plus, providing information about the potential presence of crystalline phase structures.

The surface morphology analysis of ZnO nanoparticles was conducted using a scanning electron microscope (SEM, FEI Inspect F50 FESEM, operating at an energy of 20 kV and a magnification of 5 kx). The SEM characterization was performed to observe the surface morphology and grain size of the nanomaterial. Additionally, it allowed the identification of various clusters formed by the nanoparticles.

An electrical impedance spectroscopy (EIS) test was carried out to determine the electronic conductivity of the electrolyte, utilizing the electrochemical workstation CS350. The electrochemical impedance of the ZnO electrode was measured in a 10 mM KCl mixed solution using the EIS method with a frequency range of 10 kHz to 5 MHz.

The antioxidant activity of ZnO nanoparticles as a supporting material for curcumin is evaluated using the 2,2-diphenyl-picrylhydrazyl (DPPH) assay method. The DPPH solution is 1.3 mL 1 mM DPPH concentration. The DPPH solution and 1% curcumin solution are added to a microplate containing the sample, covering the deposited ZnO. The mixture is then shaken for 10 seconds and incubated for 15 minutes before measuring its absorbance in the wavelength range of 300-500 nm. The DPPH assay method is carried out by observing the changes in absorbance after the DPPH radical reacts with the sample. The percentage inhibition is calculated using equation (1).

$$\% \mathrm{I} = \frac{\mathrm{A_0} - \mathrm{A_1}}{\mathrm{A_0}} \times 100\% \quad (1)$$

Where % I represent the percentage of inhibition, A_0 is the initial absorbance of the DPPH solution, and A_1 is the absorbance of the DPPH solution after it has reacted with the sample.

3. Results and Discussion

The XRD measurement results of ZnO nanoparticles are shown in Fig. 1. The XRD results exhibit characteristic crystallinity peaks of ZnO nanoparticles at 2θ values in the range of 0-100°. The crystal diffraction pattern of ZnO nanoparticles corresponds to the JCPDS reference number 89-1397.

Based on Figure 1, the peaks at 2θ 25.84°, 31.63°, 34.21°, and 36.12°, corresponding to the (220), (100), (002), and (101) planes, respectively. The presence of multiple peaks in all thin films indicates the random orientation of the crystallites. The analysis results reveal

that the maximum diffraction peak of ZnO is located at an angle of 25.84° with a crystal orientation of (220). This finding aligns with the research by Mousavi-Kamazani *et al.* which reported a peak at an angle of 25.12° (220), indicating the presence of $Zn(OH)_2$ in the sample. Another diffraction peak is observed at an angle of 31.63° with a crystal orientation of (100), which corresponds to the findings of Raoufi *et al.* who reported that a peak at an angle of 31.75° (100) indicating the presence of ZnO in the sample [13]. Furthermore, another diffraction peak is observed at an angle of 34.23° with a crystal orientation of (002), consistent with the results of the study by Khan *et al.* which reported a peak at an angle of 34.32° (002), indicating the presence of ZnO in the sample [14]. Additionally, there is another diffraction peak at an angle of 36.12° with a crystal orientation of (101), which aligns with the results of the study by Sohail *et al.* presented a peak at an angle of 36.15° (101), indicating the presence of ZnO in the sample [15].

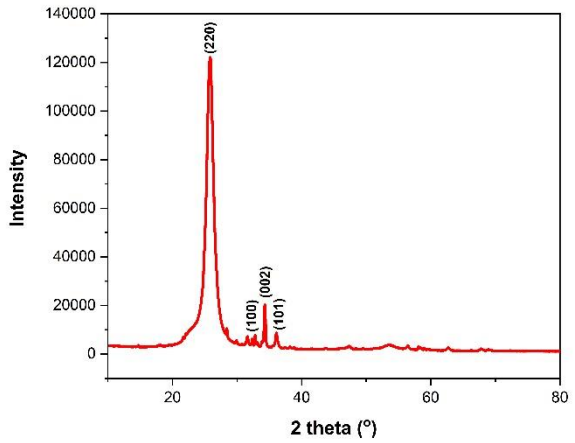

Figure 1. XRD patterns of ZnO nanoparticles deposited on the ITO substrate.

The surface morphology was obtained from the SEM results at a magnification of 5 kx, as shown in Fig. 3, where it can be observed that the produced particles have rod-shaped morphology with varying sizes. The data processing from the SEM analysis revealed the size of nanoparticles ranging from 7,16 to 73,93 nm.

The data obtained from the EIS test is presented in a Nyquist plot, where the x-axis represents real impedance or Z_{real} (Z'), and the y-axis represents imaginary impedance or Z_{imag} (Z''). The Nyquist plot matches the real part of impedance at a certain frequency range. To analyze the Nyquist plot resulting from the electrolyte test, the equivalent circuit modeling method is required, where the Nyquist plot is explained by constructing a circuit model that creates an identical plot to the test results [16]. The EIS data can be thoroughly analyzed using an equivalent circuit model consisting of circuit elements such as resistors, capacitors, Warburg impedance (W), and constant phase element (CPE).

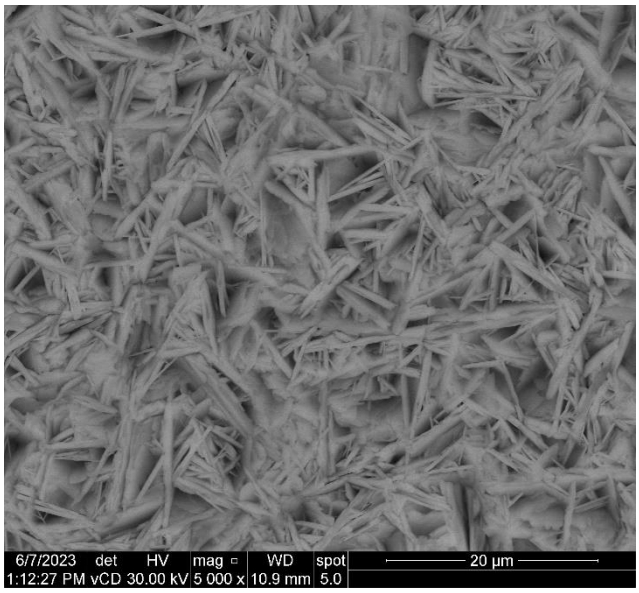

Figure 2.The results of ZnO nanoparticle SEM characterization.

Based on the results of the EIS test shown in Fig. 3, the Nyquist plots exhibit a semicircular pattern at low-frequency ranges. This semicircle is related to the values of electron resistance and charge transfer resistance (R_{ct}) of the electrode. The R_{ct} value represents the resistance associated with the working electrode (ZnO) in the system. R_{ct} provides information about the resistance occurring at the ZnO interface towards the electrolyte or its surrounding environment. Lower R_{ct} values indicate better conductivity at the electrode interface, while higher R_{ct} values indicate larger resistance at the interface. In the data, it is shown that the resulting R_{ct} value was 13.51 kΩ. This indicates that ZnO facilitates a high electron transfer from redox couples to the electrode surface [17].

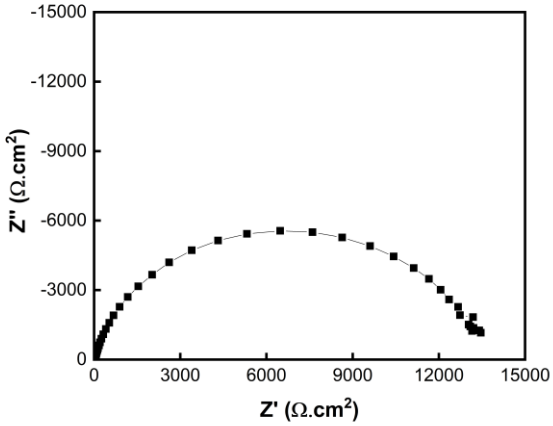

Figure 3. The Nyquist plot of the EIS test for ZnO.

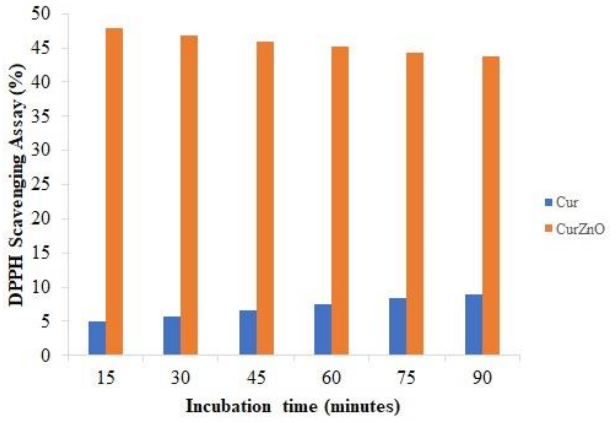

Figure 4. DPPH free radical scavenging activity of curcumin and ZnO nanoparticles-Curcumin.

The single electron present in the DPPH free radical receives a hydrogen atom donor from the phenolic group of curcumin, thus reducing the free radical [20]. The enhanced antioxidant activity of curcumin combined with ZnO is due to a coupled electron transfer reaction, where Cur-ZnO donates an electron to the free radical DPPH [21]. ZnO plays a crucial role by transferring its electron density from an oxygen atom to the unpaired electron located at the nitrogen atom within the structure of DPPH [22]. This transfer of electron density helps neutralize the DPPH radical, thereby enhancing the antioxidant activity of curcumin.

4. Conclusion

This research indicates ZnO nanoparticles synthesized using the electrodeposition method can enhance the antioxidant activity of curcumin. ZnO nanoparticles can be formed into the ITO substrate using the electrodeposition method. The EIS test shows that the Nyquist plots form a semicircle pattern in the low-frequency range. The R_{ct} value is 13.51 kΩ which is quite high and shows that ZnO can facilitate high electron transfer from the redox pair to the electrode surface. The antioxidant activity test results in the first 15 minutes, the percent inhibition of ZnO-curcumin reached 47.09% which is better if compared to cumin which was only 4.93%. This shows that ZnO increases the antioxidant activity of curcumin.

Acknowledgment

The author would like to acknowledge Badan Riset dan Inovasi Nasional (BRIN) dan Lembaga Pengelola Dana Pendidikan (LPDP) for funding this work through grant 1/RIIM II/LPPM/IV/2023.

References

[1] A. Phaniendra, D.B. Jestadi, L. Periyasamy, Free Radicals: Properties, Sources, Targets, and Their Implication in Various Diseases, *Indian Journal of Clinical Biochemistry*. **30** (2015) 11–26. https://doi.org/10.1007/s12291-014-0446-0.

[2] J. Kumar, N. Kumar, N. Sati, P.K. Hota, Antioxidant properties of ethenyl indole: DPPH assay and TDDFT studies, *New Journal of Chemistry*. **44** (2020) 8960–8970. https://doi.org/10.1039/D0NJ01317J.

[3] S.C. Lourenço, M. Moldão-Martins, V.D. Alves, Antioxidants of Natural Plant Origins: From Sources to Food Industry Applications, *Molecules*. **24** (2019) 4132. https://doi.org/10.3390/molecules24224132.

[4] H.A. Rudayni, M.H. Shemy, M. Aladwani, L.M. Alneghery, G.M. Abu-Taweel, A.A. Allam, M.R. Abukhadra, S. Bellucci, Synthesis and Biological Activity Evaluations of Green ZnO-Decorated Acid-Activated Bentonite-Mediated Curcumin Extract (ZnO@CU/BE) as Antioxidant and Antidiabetic Agents, *J Funct Biomater*. **14** (2023) 198. https://doi.org/10.3390/jfb14040198.

[5] K. Jakubczyk, A. Drużga, J. Katarzyna, K. Skonieczna-Żydecka, Antioxidant Potential of Curcumin—A Meta-Analysis of Randomized Clinical Trials, *Antioxidants*. 9 (2020) 1092.https://doi.org/10.3390/antiox9111092.

[6] M. Dei Cas, R. Ghidoni, Dietary Curcumin: Correlation between Bioavailability and Health Potential, *Nutrients*. **11** (2019) 2147. https://doi.org/10.3390/nu11092147.

[7] A.L. Lopresti, The Problem of Curcumin and Its Bioavailability: Could Its Gastrointestinal Influence Contribute to Its Overall Health-Enhancing Effects?, Advances in *Nutrition*. **9** (2018) 41–50. https://doi.org/10.1093/advances/nmx011.

[8] X. Ge, Z. Cao, L. Chu, The Antioxidant Effect of the Metal and Metal-Oxide Nanoparticles, *Antioxidants*. **11** (2022) 791. https://doi.org/10.3390/antiox11040791.

[9] R. Sharma, R. Garg, A. Kumari, A review on biogenic synthesis, applications and toxicity aspects of zinc oxide nanoparticles, *EXCLI J.* **19** (2020) 1325–1340. https://doi.org/10.17179/excli2020-2842.

[10] M.V. Arasu, A. Madankumar, J. Theerthagiri, S. Salla, S. Prabu, H.-S. Kim, N.A. Al-Dhabi, S. Arokiyaraj, V. Duraipandiyan, Synthesis and characterization of ZnO nanoflakes anchored carbon nanoplates for antioxidant and anticancer activity in MCF7 cell lines, *Materials Science and Engineering*: C. **102** (2019) 536–540. https://doi.org/10.1016/j.msec.2019.04.068.

[11] M. Bandeira, M. Giovanela, M. Roesch-Ely, D.M.

Devine, J. da Silva Crespo, Green synthesis of zinc oxide nanoparticles: A review of the synthesis methodology and mechanism of formation, Sustain *Chem Pharm.* **15** (2020) 100223. https://doi.org/10.1016/j.scp.2020.100223.

[12] Y. Liu, Z. Zhu, Y. Cheng, B. Wei, Y. Cheng, Effect of electrodeposition temperature on the thin films of ZnO nanoparticles used for photocathodic protection of SS304, *Journal of Electroanalytical Chemistry*. **881** (2021) 114945. https://doi.org/10.1016/j.jelechem.2020.114945

[13] D. Raoufi, T. Raoufi, The effect of heat treatment on the physical properties of sol–gel derived ZnO thin films, *Appl Surf Sci*. **255** (2009) 5812–5817. https://doi.org/10.1016/j.apsusc.2009.01.010.

[14] Z.R. Khan, M.S. Khan, M. Zulfequar, M. Shahid Khan, Optical and Structural Properties of ZnO Thin Films Fabricated by Sol-Gel Method, *Materials Sciences and Applications*. **02** (2011) 340–345. https://doi.org/10.4236/msa.2011.25044.

[15] M.F. Sohail, M. Rehman, S.Z. Hussain, Z. Huma, G. Shahnaz, O.S. Qureshi, Q. Khalid, S. Mirza, I. Hussain, T.J. Webster, Green synthesis of zinc oxide nanoparticles by Neem extract as multi-facet therapeutic agents, *J Drug Deliv Sci Technol*. **59** (2020) 101911.https://doi.org/10.1016/j.jddst.2020.101911

[16] H. Wang, X. Long, Y. Sun, D. Wang, Z. Wang, H. Meng, C. Jiang, W. Dong, N. Lu, Electrochemical impedance spectroscopy applied to microbial fuel cells: A review, *Front Microbiol*. **13 (**2022). https://doi.org/10.3389/fmicb.2022.973501.

[17] Y. Niu, H. Xie, G. Luo, Y. Zhuang, X. Wu, G. Li, W. Sun, ZnO-reduced graphene oxide composite based photoelectrochemical aptasensor for sensitive Cd(II) detection with methylene blue as sensitizer, Anal *Chim Acta*. **1118** (2020) 1–8. https://doi.org/10.1016/j.aca.2020.04.042.

[18] M. Ibrahim, H.N. Abdelhamid, A.M. Abuelftooh, S.G. Mohamed, Z. Wen, X. Sun, Covalent organic frameworks (COFs)-derived nitrogen-doped carbon/reduced graphene oxide nanocomposite as electrodes materials for supercapacitors, *J Energy Storage*. **55** (2022) 105375. https://doi.org/10.1016/j.est.2022.105375.

[19] F. Shahidi, Y. Zhong, Measurement of antioxidant activity, *J Funct Foods*. **18** (2015) 757–781. https://doi.org/10.1016/j.jff.2015.01.047.

[20] S. Roy, J.-W. Rhim, Carboxymethyl cellulose-based antioxidant and antimicrobial active packaging film incorporated with curcumin and zinc oxide, *Int J Biol Macromol.* **148** (2020) 666–676. https://doi.org/10.1016/j.ijbiomac.2020.01.204.

[21] S. Soren, S. Kumar, S. Mishra, P.K. Jena, S.K. Verma, P. Parhi, Evaluation of antibacterial and antioxidant potential of the zinc oxide nanoparticles synthesized by aqueous and polyol method, *Microb Pathog*. **119** (2018) 145–151. https://doi.org/10.1016/j.micpath.2018.03.048.

[22] H.A. Rudayni, M.H. Shemy, M. Aladwani, L.M. Alneghery, G.M. Abu-Taweel, A.A. Allam, M.R. Abukhadra, S. Bellucci, Synthesis and Biological Activity Evaluations of Green ZnO-Decorated Acid-Activated Bentonite-Mediated Curcumin Extract (ZnO@CU/BE) as Antioxidant and Antidiabetic Agents, *J Funct Biomater*. **14** (2023) 198. https://doi.org/10.3390/jfb14040198.